Presented at 1990 IRPS. Final

ELECTRICAL MEASUREMENTS OF MOISTURE PENETRATION THROUGH PASSIVATION

C. G. Shirley, S. C. Maston
Intel Corporation
5200 N.E. Elam Young Parkway
Hillsboro, OR 97124, USA

Abstract

The low-frequency (10KHz) dissipation factor of metal comb/serpentine structures sandwiched between a PSG substrate and passivation is a useful electrical indication of moisture penetration through the passivation. Wafer level dissipation factor readouts after periods of highly accelerated temperature/humidity testing (HAST) at 159C and 85% relative humidity were used to monitor the rate of moisture ingression through passivations of various compositions and thicknesses. For plasma-deposited oxynitride films the dominant mechanism is uniform penetration (intrinsic) with a median-time-to-failure of 370 hours (at 159/85). For oxynitride films capped by nitride films, the dominant mechanism is penetration through defects in the nitride film. The defect density of nitride cap films increases with decreasing nitride film thickness.

Introduction

Several approaches have been used to study the moisture penetration through uniform (without topography) passivation films, but little has been done on moisture penetration through passivations covering topography. McInerney and Flinn[1] used wafer bending measurements to determine the moisture diffusivity of chemical vapor deposited phosphosilicate glasses (CVD-PSG) and low-pressure, low-temperature CVD glasses (LPCVD). Their technique depends on an assumption of uniformity of the films, so that defects, such as cracks, pinholes, etc. are not a factor. They found room-temperature (23C) diffusion coefficients in the range 10^{-14} (CVD PSG) to 10^{-16} cm^2/sec (LPCVD PSG) and activation energies of 0.5 eV for these glasses. The moisture diffusion coefficients of plasma oxides and nitrides were too small to be measured using this technique, but an upper bound of 10^{-17} cm^2/sec at 23C was established. Another technique is to observe the infra-red absorption of a "sensor glass" film underlying the film of interest[2]. As moisture reaches the sensor glass, its infra-red absorption spectrum changes.

Wafer bending or infra-red absorption techniques are not suitable for passivations covering topography. Yet it is topography which is likely to dominate the moisture barrier properties of a passivation in view of the likelihood of cracks, growth seams, or other "weak spots". Our objective was to study the moisture penetration properties of passivation covering realistic topography. We used HAST[3] stressing of wafers to accelerate the penetration of moisture so that data could be obtained in a reasonable time. We used the maximum stress available to us, 159C/85% RH which, according to the model of Peck[4], can provide accelerations of 80 or so relative to 85/85. We found that 10KHz capacitance and dissipation factor (C/D) of metal combs and serpentines (providing a realistic topography) covered by passivation is a good indicator of moisture penetration. C/D is influenced by the dielectric properties and conductivities of materials above and below the metal comb/serpentines. We will show that moisture penetration through passivation is indirectly indicated by moisture-induced changes in the glass *underlying* the comb/serpentines. It should be recognized that earlier work[5,6] used changes in C/D to detect the presence of moisture on the *surface* of passivation, and thereby measure the moisture content of hermetic packages. The thermal kinetics of the effects described below ensure that we are not looking at surface effects.

Plasma nitride is known to be an excellent moisture barrier, but passivation films consisting only of plasma nitride are associated with excessive metal voiding. Plasma nitride cap films may provide the moisture barrier without the attendant metal voiding issues. We used the AC technique to study the moisture penetration properties of various plasma oxynitride passivations with and without plasma nitride cap layers, and with various thicknesses.

Experiment

We subjected wafers (or units in lidless side-brazed packages) to 159/85 HAST stress, and took periodic C/D readings on comb/serpentine structures as a function of time in stress. This was done for various passivations.

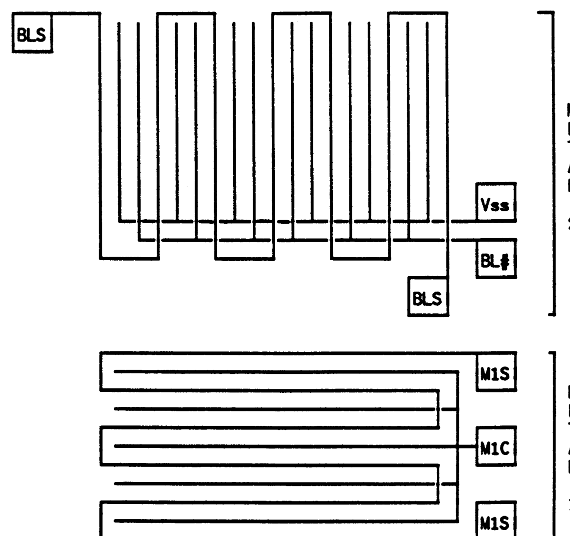

Fig. 1 Schematic of M1 and M2 comb/serpentines used in this study, not to scale. The M2 comb/serpentine overlies and is orthogonal to the M1 comb/serpentine.

Test Structure: The structure used in this experiment is generated by eliminating contacts and vias in a memory cell array and making appropriate connections at the ends of the metal lines. This results in the M2 (metal 2) and M1 (metal 1) comb/serpentine structures shown in Fig. 1. The M2 structure overlays the M1 structure and is orthogonal to it. This produces a realistic topography for the passivation to cover, except that contacts and vias are absent from the array. The structures cover an area equivalent to 8K 13μm x 17μm cells, of an SRAM array. The M2 comb/serpentine consists of two combs interleaving a serpentine so that three two-terminal measurements are possible. The M1 comb/serpentine is a single comb interleaving a serpentine so there is just one possible two-terminal measurement. The test die containing this structure is repeated at 74 locations across a 150mm wafer.

Electrical Measurements: AC C/D measurements were carried out on 74 test sites on each wafer, and on some packaged units assembled in lidless side-brazed packages. The data were acquired using a Hewlett-Packard 4275A LRC meter connected through a Keithley 707 switching matrix to either a socket or to special shielded probes on an Electroglas 2010X automatic prober. The LRC meter can be set to a mode which directly displays and transmits C and D.

C and D was acquired for the three possible two-terminal connections to the M2 comb/serpentine at several frequencies. We found that the dissipation factors measured in each of the three ways gave similar results, so only one (between BLS and Vss in Fig. 1) will be reported in this paper. For this measurement, the unused terminal and the substrate were grounded. For M1 the one possible C and D measurement was made with the substrate grounded.

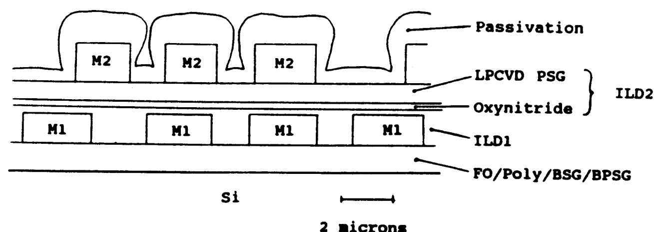

Fig. 2 Schematic cross-section of part of the test array used in this experiment.

Materials: The materials used in this experiment were fully processed wafers, or dice mounted in open-lidded side-brazed packages. A simplified cross-section is shown in Fig. 2. M1 is deposited and patterned on a reflowed boro-phospho-silicate glass (BPSG) substrate. M2 is isolated from M1 by an inter-layer dielectric (ILD) that is formed in two steps. The first part, ILD1, is a planarized plasma oxynitride. The second part, ILD2, is deposited on the resulting planar substrate. ILD2 consists of 0.15μm of oxynitride under 0.6μm of LPCVD PSG. After M2 deposition and patterning, a conformal plasma-deposited passivation is deposited, and the bond pad openings are cleared. The passivation was varied by using several single layer and composite plasma-deposited films shown in Table I. The films ranged from oxide (refractive index 1.6) through oxynitride (refractive index 1.75), to nitride (refractive index 2.1).

Data presented in this paper were acquired from 3 lots and 7 wafers. Within-lot processing was identical except for the passivation which was varied. Wafers from lot 1 were used to understand and optimize the technique, while wafers from lots 2 and 3 were used to explore the effects of different passivations.

Table I. List of materials studied.

Lot	Wafer	Passivation
1	21*	1.0μm oxynitride
1	25	1.0μm oxynitride
2	36	0.05μm ox/0.8μm oxynit/0.2μm nitride
2	37	0.05μm ox/0.8μm oxynit/0.1μm nitride
2	47	1.0μm oxynitride
3	11	0.05μm ox/0.3μm oxynit/0.2μm nitride
3	30	0.05μm ox/0.8μm oxynit/0.2μm nitride

Note: * Data acquired at package level.

Environmental Stress: Wafers or packaged units were generally subjected to 40 hours of unbiased 159/85 HAST stress, then removed and tested within 8 hours. This was repeated many times to acquire C/D as a function of accumulated stress time. Sometimes delays of up to 100 hours occurred before returning units to stress, but this had little effect on the accumulation of stress times because of the high acceleration of the stress. See also the data on bake-out and bench recovery below.

Results

Sensitivity of C vs D and M1 vs M2 to HAST Stress: Figure 3 gives the 100KHz capacitance and dissipation factor distributions for M2 comb/serpentine and M1 comb/serpentine for wafer 25, from lot 1, (with 1μm of oxynitride passivation) as a function of time in 159/85 HAST. Two observations may be made:

- Dissipation factor is a much more sensitive indicator of moisture penetration than capacitance. (Compare Fig. 3 top left with Fig. 3, top right. Note the scales; D changes by a factor of 5 or more, whereas C changes only by at most 20%.) We shall see below that this effect is more pronounced at lower frequencies.

- M1 comb/serpentine C and D are insensitive to moisture penetration (Fig. 3, bottom).

The M2 dissipation factor is the parameter most sensitive to HAST-induced changes. Therefore, the discussion will center on the M2 dissipation factor in the remainder of this paper.

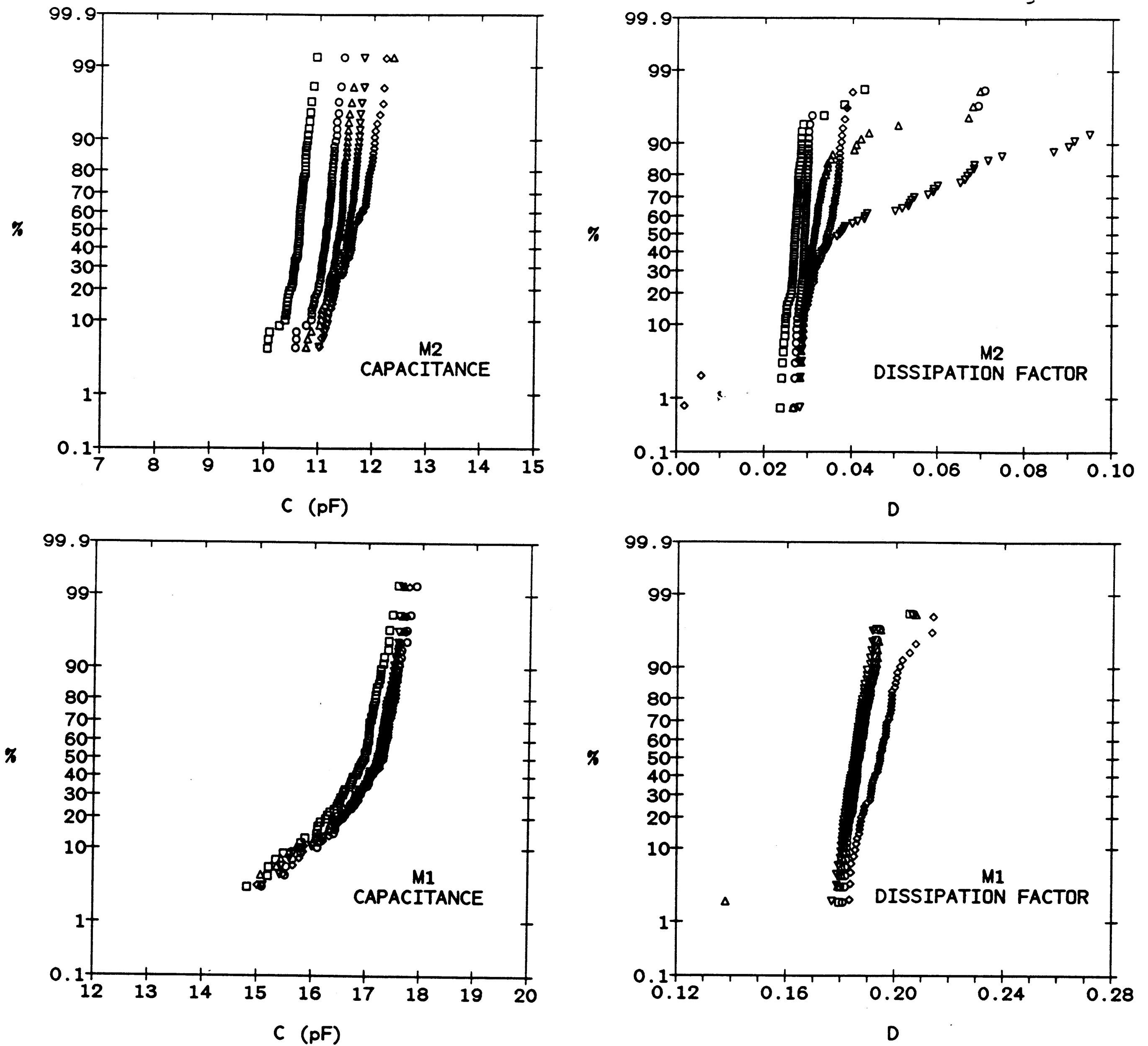

Fig. 3 Distributions of 100KHz capacitance and dissipation factors as a function of time (hours) in 159/85 HAST for wafer 25 of lot 1. This wafer is passivated by 1μm of plasma oxynitride.

□	0	▽	200
○	80	◇	280
△	160		

<u>Spatial Distribution and Time Dependence of Changes in M2 Dissipation Factor</u>: The M2 dissipation factor data (top right, Fig. 3) shows that moisture penetrates passivation at different locations on the wafer at different times. The 200-hour 159/85 data from top right, Fig. 3, are shown as a wafer map in Fig. 4. Areas which are relatively unchanged have an hour-glass shaped distribution.

Dissipation factors along the cross section indicated in Fig. 4 are shown as a function of stress time in Fig. 5. Up to 120 to 150 hours of 159/85 HAST, only small changes in D are seen. After 150 hours, some of the dice show large shifts in D, while others don't. Moreover, dice which are strongly affected show an increase, then a decrease, in dissipation factor as a function of stress time.

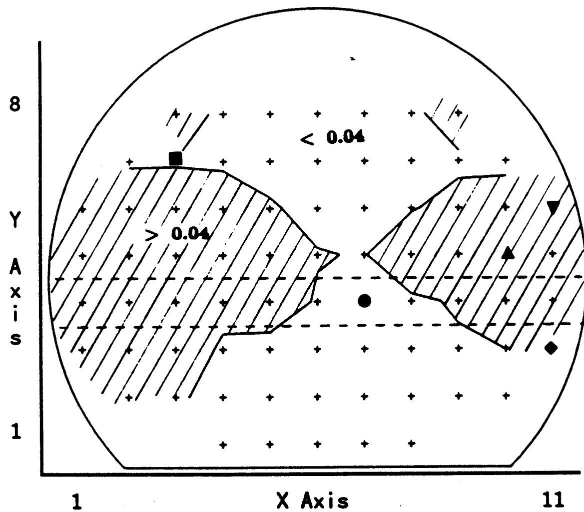

Fig. 4 Wafer map of wafer 25, lot 1, (data from top right, Fig. 3) 100KHz dissipation factor after 200 hours of 159/85 HAST. Symbols indicate sites for which detailed frequency data are plotted in Fig. 6.

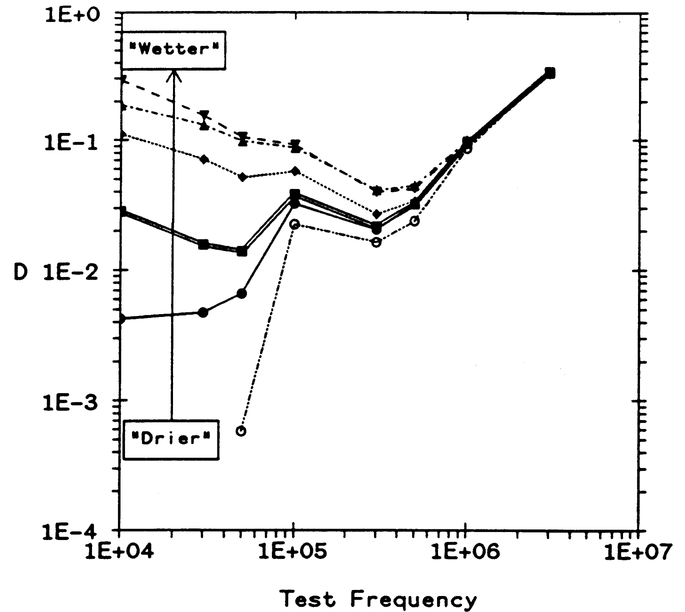

Fig. 6 M2 dissipation factor vs frequency for dice variously affected by moisture at the 200 hour 159/85 readout of wafer 25, lot 1. Dice chosen are indicated in Fig. 4. Also shown (open circle) are data from a die from an unstressed wafer (wafer 30, lot 3).

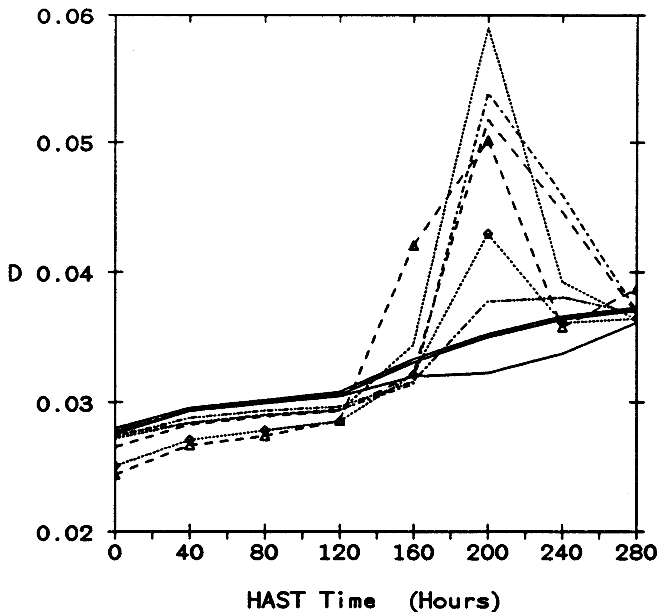

Fig. 5 Time evolution at 159/85 HAST of M2 100KHz dissipation factors from the section shown in Fig. 4 from wafer 25, lot 1. (X,Y coordinates refer to sites on wafer map in Fig 4.)

(2,4)
(3,4)
(4,4)
(5,4)
(6,4)
(7,4)
(8,4)
(9,4)

Frequency Dependence of M2 Moisture-Induced Changes in Dissipation Factor: We studied the frequency dependence of the dissipation factor on the 200-hour readout of wafer 25 of lot 1, which we knew to have dice variously affected by moisture (as shown in Fig. 4). The data are shown in Fig. 6. Added to the plot are D vs f data for an unstressed wafer from another run, with a different passivation (lot 3, wafer 30). We observe:

- o The maximum sensitivity to moisture penetration is at the lowest frequency available, 10KHz. Above 300KHz there is little sensitivity to moisture.
- o There is a peak in dissipation, unrelated to moisture, at 100KHz. Below 100KHz, dissipation factors for "dry" test sites are very close to zero.
- o The slope of the log D vs log f plot is -0.5 at low frequency, once moisture begins to affect the die.

Bake-out Recovery: Wafer 25 from lot 1 was accidentally destroyed before a bake-out recovery experiment could be done. However, bake-out data were acquired in an earlier experiment using another wafer from the same lot (wafer 21) with identical processing. This wafer was assembled into lidless side-brazed packages and stressed in 159/85 HAST. Dissipation factor data were acquired at 100KHz as a function of increasing time in 159/85 HAST. Different dice showed different shifts in D as a function of stress time. This is shown in Fig. 7 (left side). Notice the characteristic increase, then decrease, in D. This was observed earlier in dissipation factor data in Fig. 5. The small negative offset in D at early stress times is caused by instrumental error.

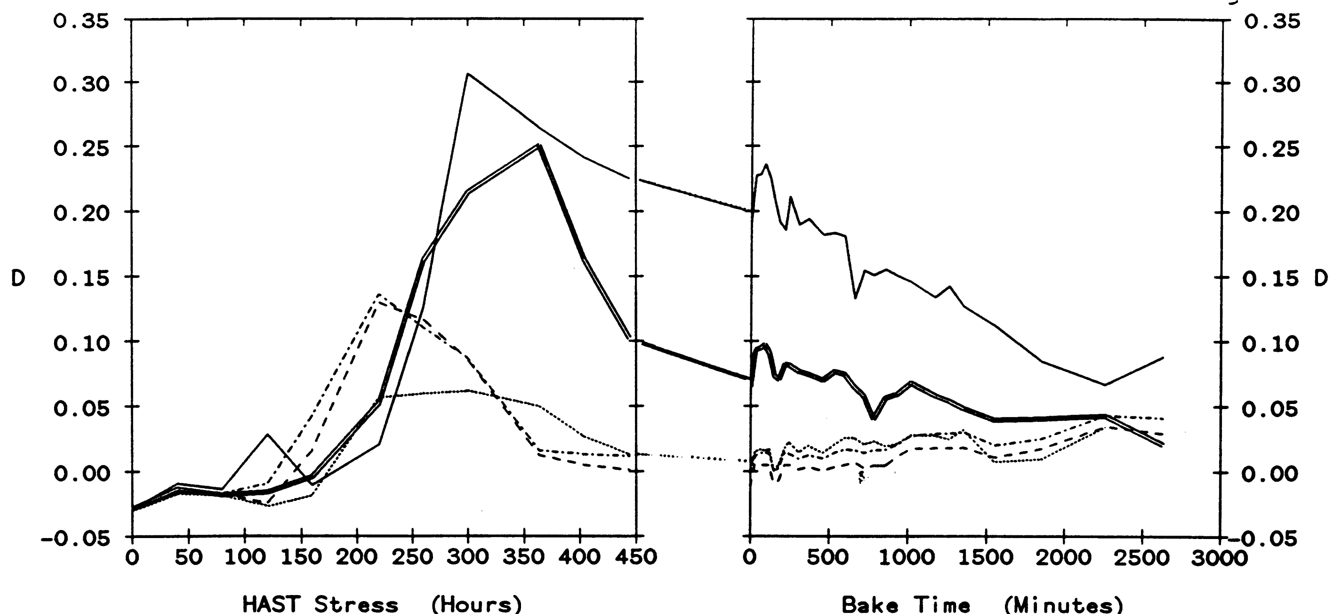

Fig. 7 Saturation and bake recovery of M2 100KHz dissipation factor of several units from wafer 21 of lot 1. Left: Changes in D during 159/85 HAST. Right: Recovery during 160C bake. Two weeks elapsed between the end of HAST stress and the beginning of the bake recovery test.

After a two-week delay at room ambient during which little change was seen, a series of 160C bakes was started. The recovery characteristics at 160C are shown on the right side of Fig. 7. Significant, but not complete, recovery was observed.

Effect of Various Passivations: Lots 2 and 3 were used to compare various triple-layer passivations and a 1μm oxynitride passivation, as shown in Table I. The 0.05μm plasma oxide underlayer on the triple layer passivations probably has little effect. All dissipation factor data in this experiment were taken at 10KHz to maximize the sensitivity to moisture-induced changes.

The effect of replacing the top 0.2μm of oxynitride with a nitride cap, and then reducing the nitride cap thickness to 0.1μm (lot 2), is shown in Fig. 8. The effect of reducing the thickness of the oxynitride middle layer in a triple-layer sandwich (lot 3) is shown in Fig. 9. The small negative offset in D at early stress times is instrumental error.

The data in Figs. 8 and 9 show the differing moisture penetration characteristics of the various passivations, but further analysis provides more information. We set an arbitrary failure criterion of $D_{crit} = 0.005$. It is not known how this criterion relates to actual device failure. For each test site we recorded the accumulated stress time at which D first exceeded D_{crit}. For a given test site, any data later than this time are ignored, even though D will later fall below D_{crit}. Also, sites which exceeded D_{crit} at zero stress time were not included in the analysis. The distributions of failure times for wafers from lot 2 and lot 3 are shown in Figs. 10 and 11, respectively.

The distribution of failure times for the 1μm oxynitride film (lot 2, wafer 47) is characterized by a lognormal distribution with $t_{50} = 370$ hours and $\sigma = 0.27$ (based on natural logarithms). A wafer map of the times to $D > D_{crit}$ is shown in Table II. It is apparent that many sites fail simultaneously at about 400 hours over a wide area of the wafer. This, and the small value of σ, indicate that the penetration mechanism is not a result of defects, but is intrinsic to the oxynitride film.

The failure times for the passivation film with the 0.1μm nitride cap (wafer 37, lot 2) also has a lognormal distribution (Fig. 10), but with a larger value of t_{50} and σ ($t_{50} = 790$ hours, $\sigma = 0.46$). A wafer map of times to $D > D_{crit}$ is shown in Table III. Most of the early failures in Table III are in the periphery of the wafer. This, and the larger value of σ, indicate that a defect mechanism may be responsible for the failures.

These observations led us to look for the defects responsible for the early failures on the 0.1μm nitride cap passivation (wafer 37, lot 2). We made a post-742-hour HAST SEM survey of this wafer for cracks in the passivation which could be correlated to test sites with large dissipation factor changes. We saw crazing in the passivation at test sites with and without large shifts in D. It should be recognized that the narrow pitch of the metal lines made it impossible to survey directly the base of the M2 lines, which is a likely site for a crack. We also took dice from areas of the wafer exhibiting large and small post-HAST shifts in D and looked for passivation thickness differences in cross section. Again, we could find no correlation. Finally, we subjected the dice to a quick-kill solution[7] which will enter cracks in the passivation and etch metal. Etched spots in the metal are easy to observe, and counts of them are an indication of passivation defect density. The quick-kill solution was aggressive and etched large areas of the array we actually used to make the

Table II. Hours in 159/85 HAST until D (10KHz) > 0.005 for a $1\mu m$ oxynitride passivation (wafer 47, lot 2). Missing sites failed at the initial test.

		>462	462	400	400	400	280			
	400	360	400	400	400	400	360	280	240	
240	280	320	320	360	400	400	360	320	280	160
240	320	360	400	360	400	400	360	360	320	320
240	320	360	400	400	400	400	400	400	360	360
280	320		400	462	462	>462	462	>462	240	160
	320		462	462	>462	>462	160	>462	462	
				>462	>462	>462	>462			

Flat

Table III. Hours in 159/85 HAST until D (10KHz) > 0.005 for a $0.05\mu m$ oxide/$0.8\mu m$ oxynitride/$0.1\mu m$ nitride passivation (wafer 37, lot 2).

		120	400	400	360	240	320			
	742	542	542	582	582	582	502	462	>742	
>742	>742	>742	>742	>742	>742	>742	>742	542	502	>742
>742	>742	>742	>742	>742	>742	>742	>742	>742	542	>742
>742	>742	742	742	>742	742	>742	>742	>742	542	>742
>742	>742	>742	>742	>742	>742	>742	>742	662	462	>742
	662	742	582	662	>742	502	502	400	462	
			>742	742	662	662	582			

Flat

Table IV. Quick-Kill Counts after 742 Hours of 159/85 HAST on wafer 37, lot 2.

		-	100	69	-	>100	-			
	83	83	74	-	-	>100	>100	>100	>100	
77	23	12	2	2	10	32	28	70	-	80
3	6	1	0	1	1	2	12	50	82	51
4	1	0	-	-	3	6	-	67	49	-
25	10	9	2	1	3	1	11	-	92	-
	20	22	-	44	51	78	88	>100	56	
			-	86	>100	-	-			

Flat

Note: "-" indicates dice removed for other tests.

electrical measurements, but a different adjacent array was less susceptible and meaningful counts could be made. A map of the quick-kill counts is shown in Table IV. This table has the same orientation as the wafer map in Table III, and the same C-shaped pattern is apparent.

From Figs. 10 and 11 we see that the failure time distributions for all of the $0.2\mu m$ nitride cap passivations (Table I) have very large values of σ (about 3). The failures occur at a few peripheral sites. This indicates that moisture penetrates the passivation only at defects. From Fig. 11 it can be seen that the $0.2\mu m$ nitride cap film with a $0.3\mu m$ oxynitride underlayer has a significantly higher defect density than the $0.2\mu m$ nitride cap film with a $0.8\mu m$ oxynitride underlayer.

Discussion

The observations support a model in which moisture slowly penetrates the passivation uniformly or through defects and then diffuses rapidly over distances of the order of $1\mu m$ through the underlying PSG to create a leakage path between M2 comb and serpentine. From the results of Ref. 1, moisture will take about 10 hours to diffuse $1\mu m$ in CVD PSG at 159C. On the other hand, the observed incubation times (times before the onset of changes in D) at 159/85 range within a wafer from 150 hours to 500 hours in the case of oxynitride, and from 300 hours to more than 750 hours for nitride-capped passivations. This indicates that moisture penetration through the passivation is the rate-limiting step. When moisture reaches the PSG, it is hydrolyzed producing hydronium and phosphate ions[8] which locally increase the conductance between M2 lines. With further exposure to HAST stress, however, the conductance decreases due to the eventual formation of a surface oxide barrier on the aluminum, limiting, then reducing, the conductance between metal lines[9]. The oxynitride film underlying the PSG provides a moisture barrier and electrical isolation so that M1 is not provided with a low resistance shunt through the PSG as PSG becomes affected by moisture. Therefore, the M1 comb/serpentine C/D is much less affected by HAST stress. The existence of a moisture-induced low-resistance shunt to the M2 comb/serpentine capacitance is supported by the frequency dependence of D at low frequency. For a capacitance, C, shunted by a resistance, R, D is given by $D=(2\pi fRC)^{-1}$ so that a logarithmic plot of D versus f should have a slope of -1. This is the expected behavior in the low frequency limit at frequencies less than resonant frequencies due to polarization.[10] In Fig. 6, the proximity of the resonance near 100KHz makes the slope closer to -0.5 rather than -1.

The bench and bake-out recovery results are explained as follows: Once moisture enters through a defect in the passivation, it will disperse by relatively rapid horizontal diffusion in the PSG, rather than by loss through the passivation. This will effect a local "drying" which will reduce the conductance between M2 lines. Thus the recovery kinetics are governed by the moisture diffusion kinetics of PSG. At room temperature (assuming a diffusion coefficient of 10^{-15} cm^2/sec) it takes moisture 3000 hours to diffuse $1\mu m$ (see Ref. 1), so C/D will take weeks

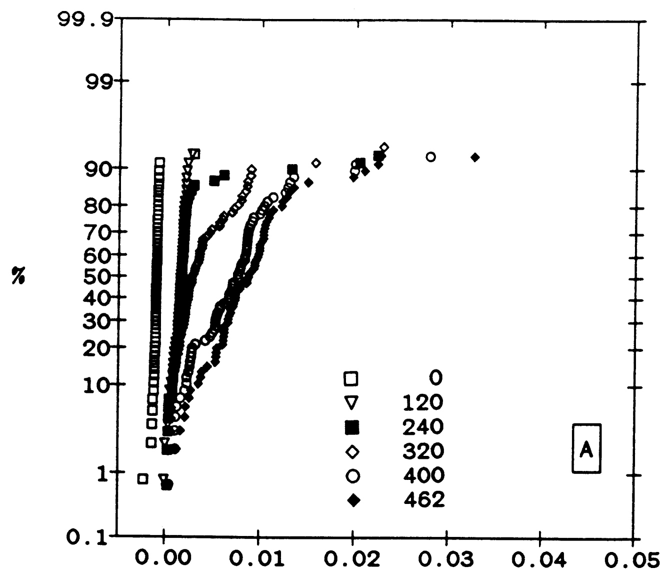

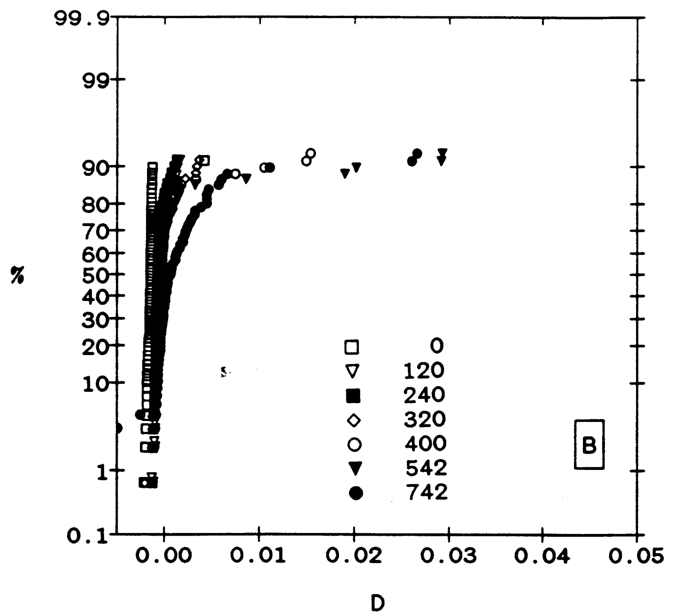

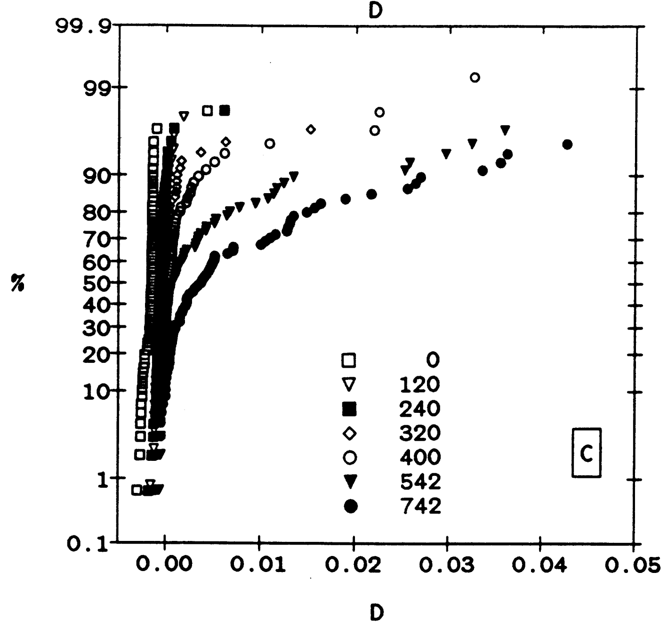

Fig. 8 Distributions of 10KHz dissipation factor for wafers from lot 2 as a function of time (hours) in 159/85 HAST.

A: Wafer 47 with 1μm of plasma oxynitride.

B: Wafer 36 with a composite film of 0.05μm oxide/0.8μm oxynitride/0.2μm nitride.

C: Wafer 37 with a composite film of 0.05μm oxide/0.8μm oxynitride/0.1μm nitride.

to change on the bench. On the other hand, a moisture diffusion activation energy of 0.5eV implies that changes at 160C will occur in a few hours. This is confirmed by the results shown in Fig. 7. The bench and bake-out kinetics indicate that the conduction mechanism is not related to changes on the surface of the passivation. Such surface changes (such as condensation, etc.) would recover on a time scale of seconds and minutes, not hundreds and thousands of hours.

For a 1μm plasma oxynitride film, we saw an intrinsic moisture penetration mechanism with a median-time-to-fail in 159/85 HAST of 370 hours. Using elementary diffusion theory, this implies a diffusion coefficient of about 7 x 10^{-15} cm^2/sec at 159C for plasma oxynitride. When the oxynitride is capped by a plasma nitride film, the distributions of D do not move uniformly to longer times, but become strongly bimodal, indicating that moisture penetration is through defects in the cap film. As the nitride cap layer becomes thinner, the defect density increases. The distribution of these defects is not random, but shows a pattern probably related to some process parameter. We could not easily observe the defects, but their existence was confirmed by a quick-kill technique. We could not determine the intrinsic moisture penetration rates of plasma nitride films. For defect-free test sites, even a 0.1μm film of plasma nitride was sufficient to prevent moisture-induced changes even after 742 hours of 159/85 HAST. This places an upper bound of 4 x 10^{-17} cm^2/sec at 159C on the plasma nitride moisture diffusion coefficient.

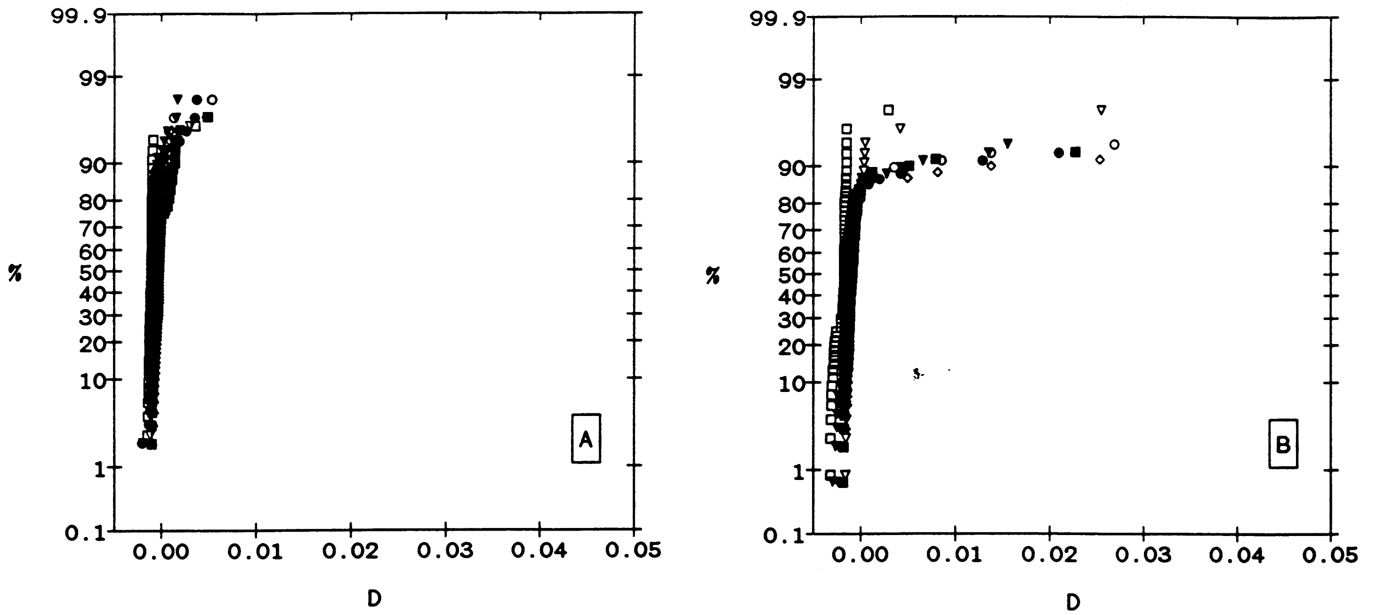

Fig. 9 Distributions of 10KHz dissipation factor for wafers from lot 3 as a function of time (hours) in 159/85 HAST.

A: Wafer 30 with a composite film of 0.05μm oxide/0.8μm oxynitride/0.2μm nitride.

B: Wafer 11 with a composite film of 0.05μm oxide/0.3μm oxynitride/0.2μm nitride.

□ 0
▽ 120
■ 240
◇ 320
○ 400
▼ 542
● 742

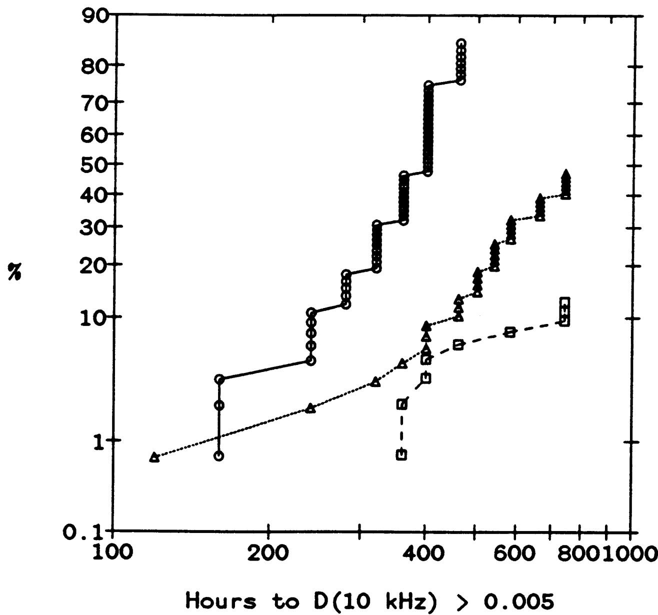

—○— Wafer 47. 1 micron oxynitride
--□-- Wafer 36. 0.05 ox/0.8 oxynit/0.2 nit
····△···· Wafer 37. 0.05 ox/0.8 oxynit/0.1 nit

Fig. 10 Distribution of times to $D > D_{crit}$ in 159/85 HAST stress for wafers from lot 2. Shows the effect of replacing the top 0.2μm of a 1μm oxynitride film with 0.2μm of nitride, and with 0.1μm of nitride.

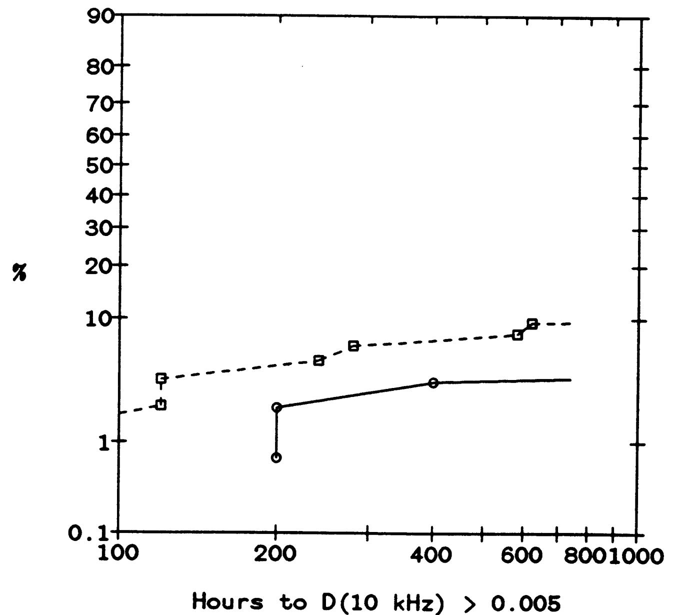

—○— Wafer 30. 0.05 ox/0.8 oxynit/0.2 nit
--□-- Wafer 11. 0.05 ox/0.3 oxynit/0.2 nit

Fig. 11 Distribution of times to $D > D_{crit}$ in 159/85 HAST stress for wafers from lot 3. Shows the effect of reduction of oxynitride middle layer thickness in 0.05μm oxide/oxynitride/0.2μm nitride from 0.8μm to 0.3μm. The difference between curves is significant at 60% confidence level.

Conclusions

- For a 1μm oxynitride passivation the moisture ingression mechanism is uniform penetration with a median-time-to-failure of 370 hours and $\sigma = 0.37$ in 159/85 HAST. This corresponds to a moisture diffusion coefficient of 7×10^{-15} cm^2/sec at 159C.
- Moisture penetration through nitride-capped oxynitride passivations is dominated by non-uniformly distributed local defects which are very difficult to identify visually. The weak spots are still relatively good moisture barriers, with 95% of the test sites surviving 200 hours or longer in 159/85, even for the 0.1μm nitride cap passivation.
- As nitride cap thickness decreases, the defect density increases.
- The intrinsic moisture penetration rates for plasma nitride were too low to be measured, but an upper bound on the moisture diffusion coefficient was determined to be 4×10^{-17} cm^2/sec at 159C.
- Moisture penetration through passivation locally hydrolyzes PSG and causes local increases in conductivity between M2 lines. The increases in conductivity are "frozen-in" at room temperature and are conveniently detected at the wafer level by low-frequency (about 10KHz, or less) dissipation factor measurements.
- Dissipation factor measurements combined with HAST stress at the wafer level are a useful alternative to the traditional quick-kill determinations of passivation film integrity. The test is not as destructive and the result relates directly to the temperature-humidity life of the passivation film. Moreover, tedious visual counting is avoided.

Acknowledgments

Thanks are due to Don Danielson and Des Chatigny for HAST support, to Mike McKeag and Mary Cavitt for support with SEM work, and to Melton Bost and Roberta Angell for providing the quick-kill testing.

References

1. E. J. McInerney and P. A. Flinn, "Diffusivity of Moisture in Thin Films," in Proc. 20th Ann. Int'l Reliability Physics Symposium, pp. 264-267, (1982).
2. K.S. Daghir, "Method of Measuring Moisture Transmission Through Protective Coatings and Passivation Layers," Abstract of Electro. Chem. Soc. Meeting, Abs. No. 268, (1972).
3. J. E. Gunn, S. K. Malik, P. M. Mazumdar, "Highly Accelerated Temperature and Humidity Stress Technique (HAST)," in Proc. 19th Ann. Int'l Reliability Physics Symposium, pp. 48-51, (1981).
4. D. S. Peck, "Comprehensive Model for Humidity Testing Correlation," in Proc. 24th Ann. Int'l Reliability Physics Symposium, pp. 44-50, (1986).
5. R. P. Merrett, S. P. Sim, J. P. Bryant, "A Simple Method of Using the Die of an Integrated Circuit to Measure the Relative Humidity Inside Its Encapsulation," in Proc. 18th Ann. Int'l Reliability Physics Symposium, pp. 17-25, (1980).
6. S. L. Garveric and S. D. Senturia, "An MOS Device for AC Measurement of Surface Impedance with Application to Moisture Monitoring," IEEE Transactions on Electron Devices, Vol. ED.29, pp. 90-94, (1982).
7. The quick-kill solution consists of two solutions A and B combined just before the test. Solution A is a 50/50 solution of 0.2M KOH and Clorox bleach (5.25 wt% NaOCl), while solution B is a 30% solution of hydrogen peroxide. The dice were immersed in a 75C mixture of solutions A and B for 15 minutes.
8. W. M. Paulson and R. W. Kirk, "The Effects of Phosphorus-doped Passivation Glass on the Corrosion of Aluminum," in 12th Ann. Proc. Int'l Reliability Physics Symposium, p. 172, (1974).
9. V. Bhide, J. M. Eldridge, "Aluminum Conductor Line Corrosion," in 21st Ann. Proc. Int'l Reliability Physics Symposium, pp. 44-51, (1983).
10. L. I. Maissel and R, Glang, eds., Handbook of Thin Film Technology. New York, McGraw-Hill, 1970, Ch. 16, pp. 16-11 to 16-15.

Fig 2. Capacitance and Dissipation Factors at 100KHz vs Time at 159/85 HAST, Run 15-820, Wafer 10. Oxynitride ILD2, Oxynitride passivation.

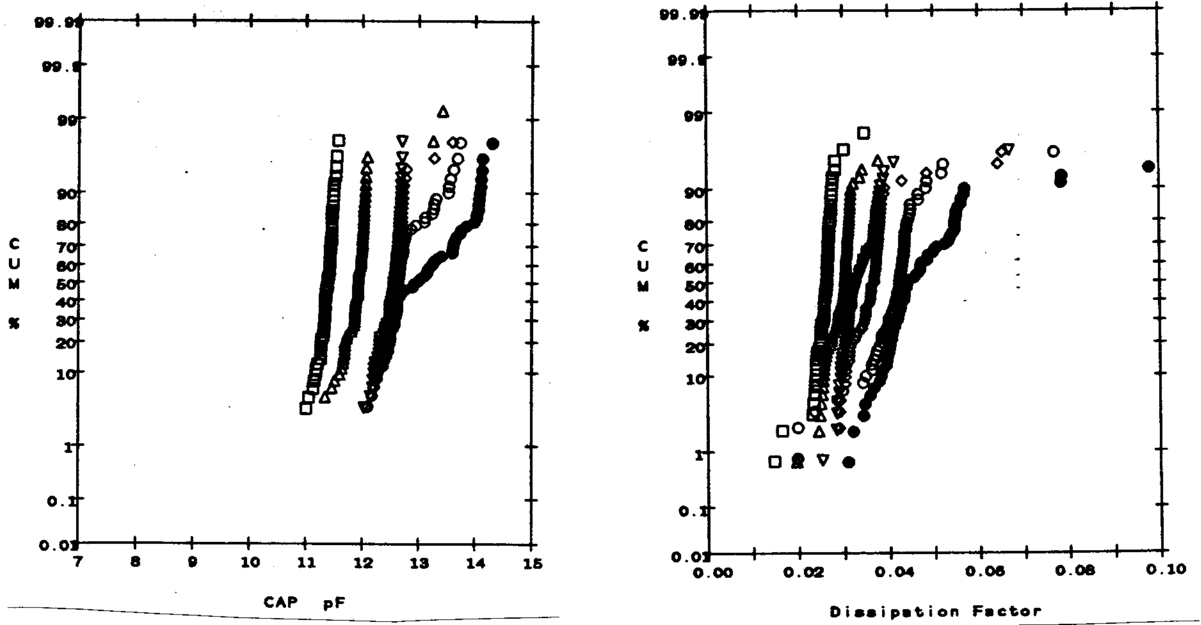

Metal 2 Array Defect Monitor
Vss / Serpentine

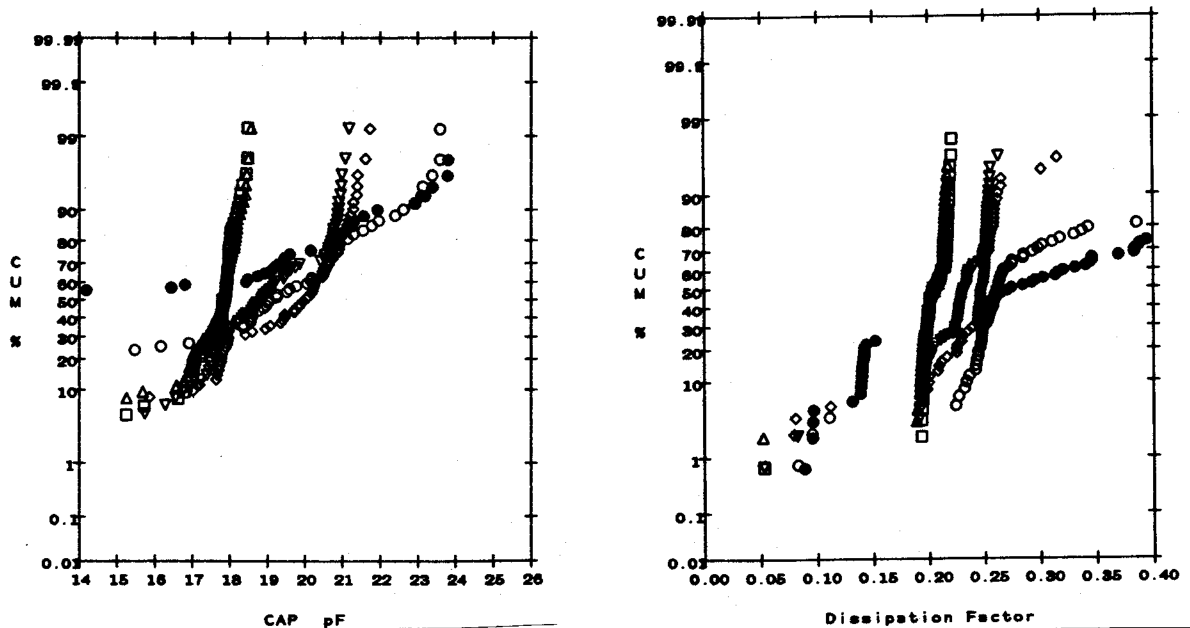

Metal 1, Array Defect Monitor
M1 Comb / M1 Serpentine

□ Pre-Stress.
△ HAST 204 Hrs.
▽ HAST 404 Hrs.
◇ HAST 524 Hrs.
○ HAST 644 Hrs.
● HAST 724 Hrs.

Fig 4. Comparison of 10KHz dissipation factors measured in two ways on M2 ADM. 240 hour 159/85 readout of wafer 25, run 15-820.

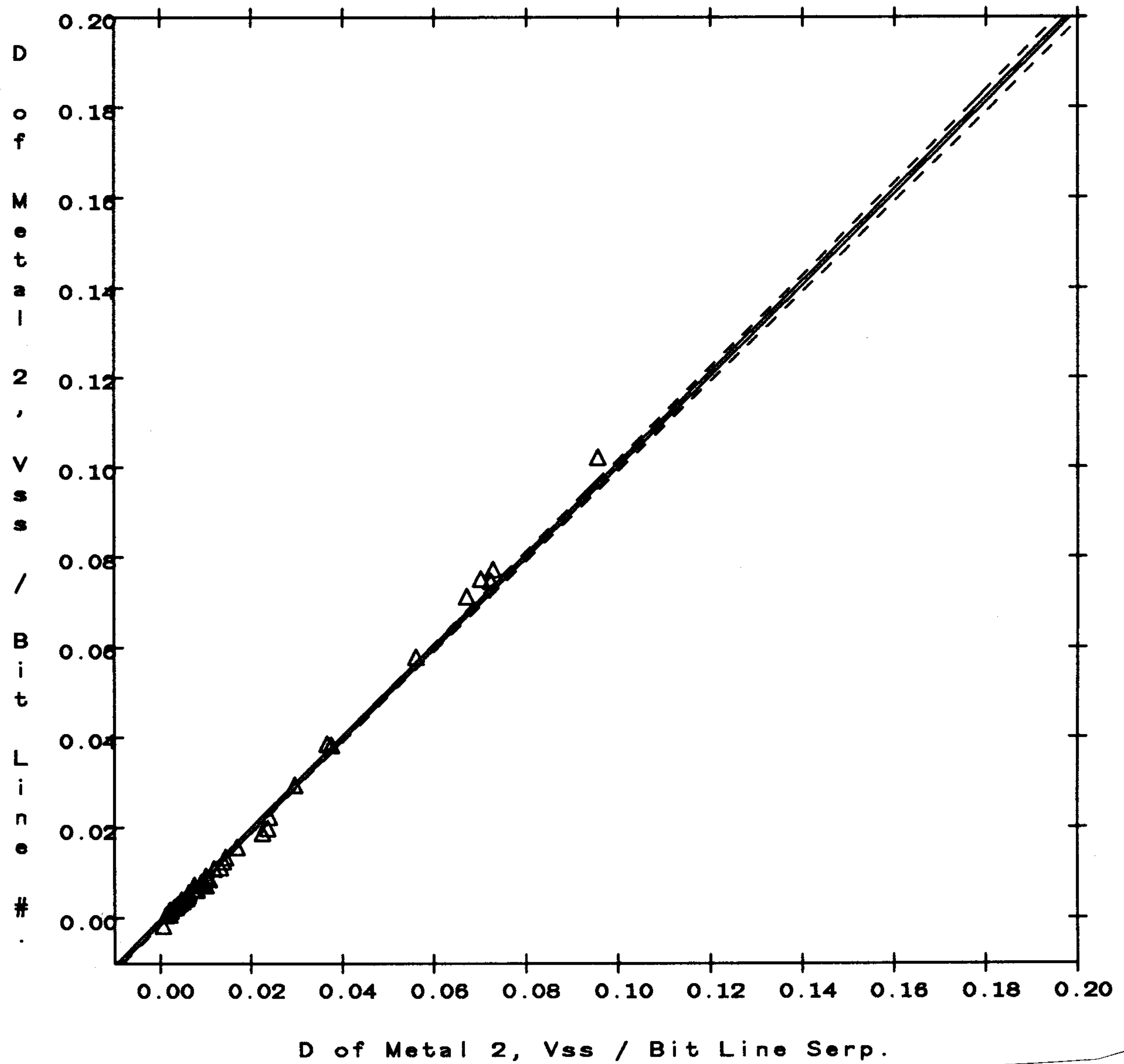

Fig 9. Dissipation Factors at 10KHz
Vss / Bit Line Serp vs Time at 159/85 HAST
Triple-layer passivations.

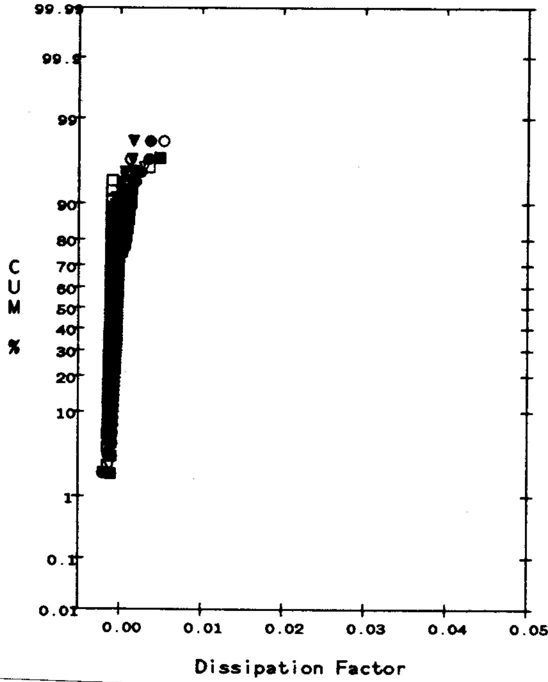

Run 29-841, Wafer 30
0.05 Ox + 0.8 Oxy + 0.2 Nitride

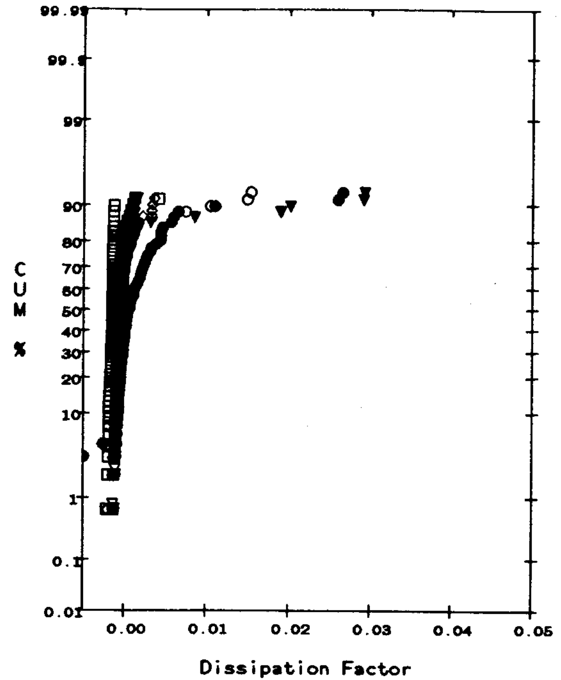

Run 26-833, Wafer 36
0.05 Ox + 0.8 Oxy + 0.2 Nitride

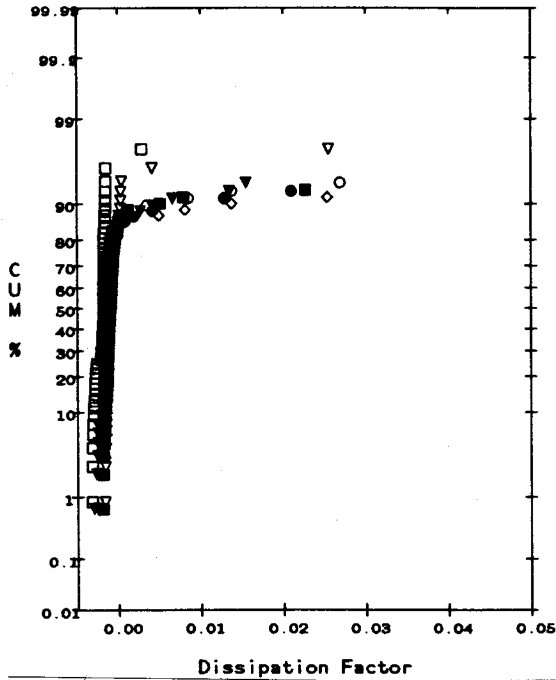

Run 29-841, Wafer 11
0.05 Ox + 0.3 Oxy + 0.2 Nitride

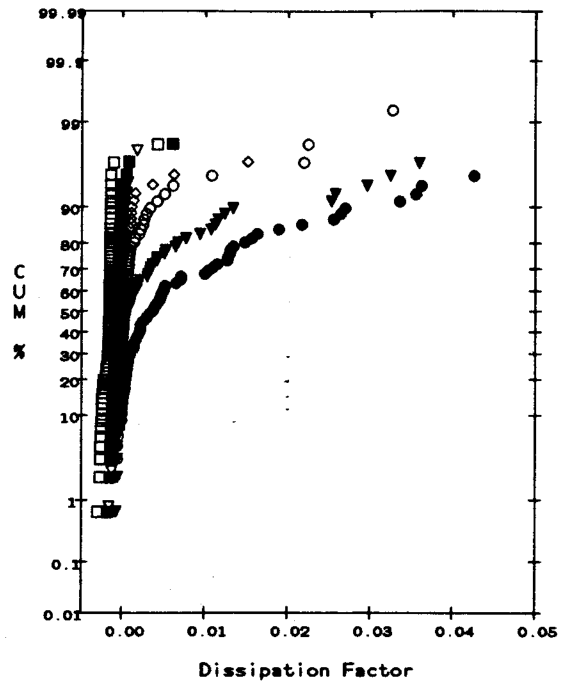

Run 26-833, Wafer 37
0.05 Ox + 0.8 Oxy + 0.1 Nitride

□ Pre-Stress
▽ HAST 120 Hrs.
■ HAST 240 Hrs.
◇ HAST 320 Hrs.
○ HAST 400 Hrs.
▼ HAST 542 Hrs.
● HAST 742 Hrs.

Fig 10. Dissipation Factors at 10KHz
Vss / Bit Line Serp vs Time at 159/85 HAST
Run 26-833, Wafer 47.
Passivation: Oxynitride (1u).

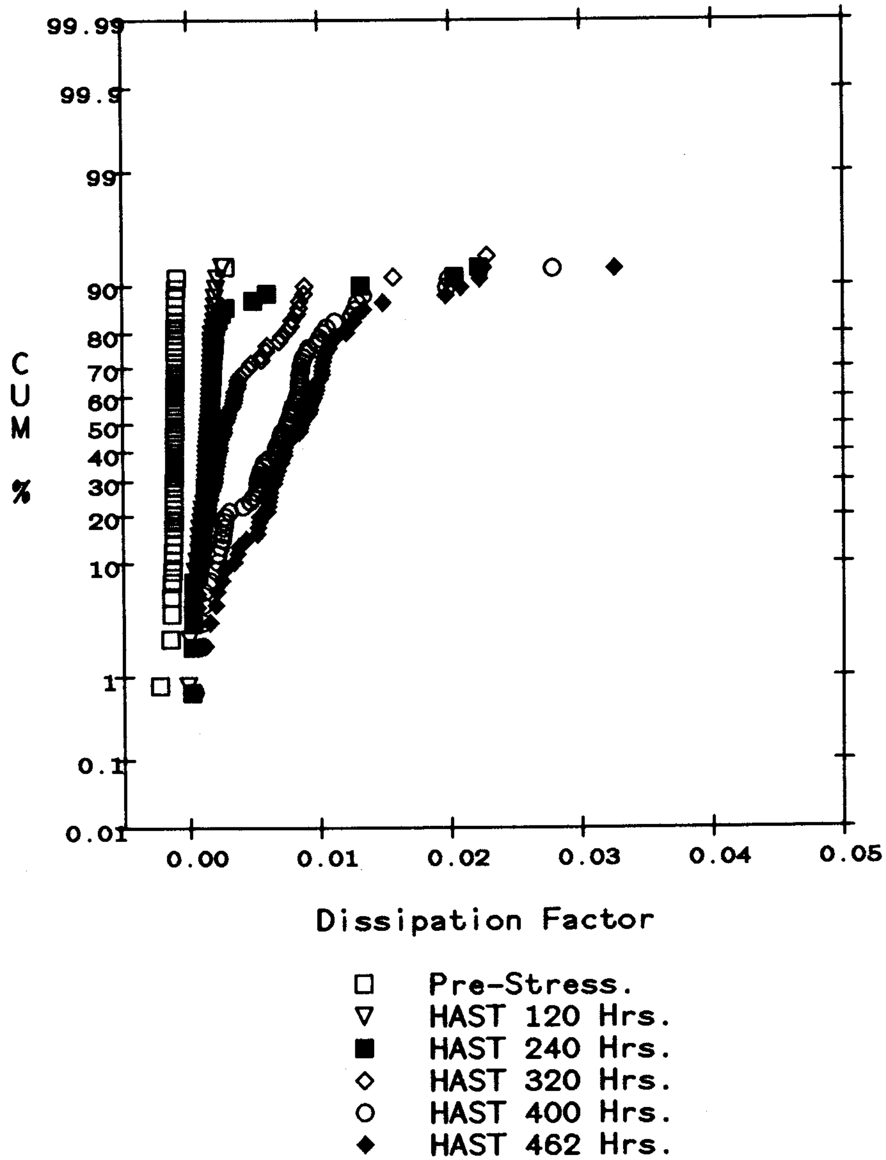

Fig 12. Time dependence of 10KHz dissipation factor for dice on section of wafer 37, run 26-833, shown in Fig. 11.

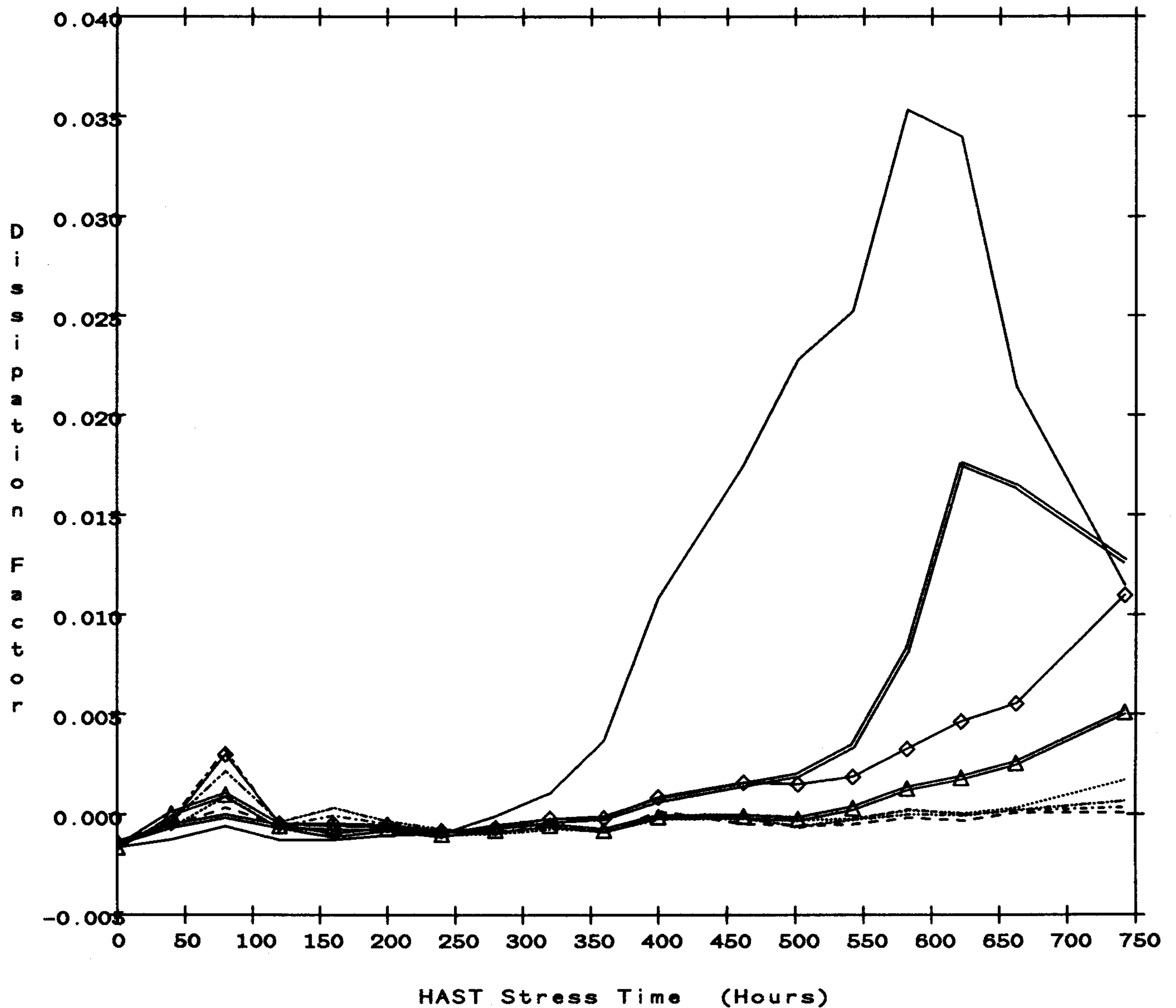

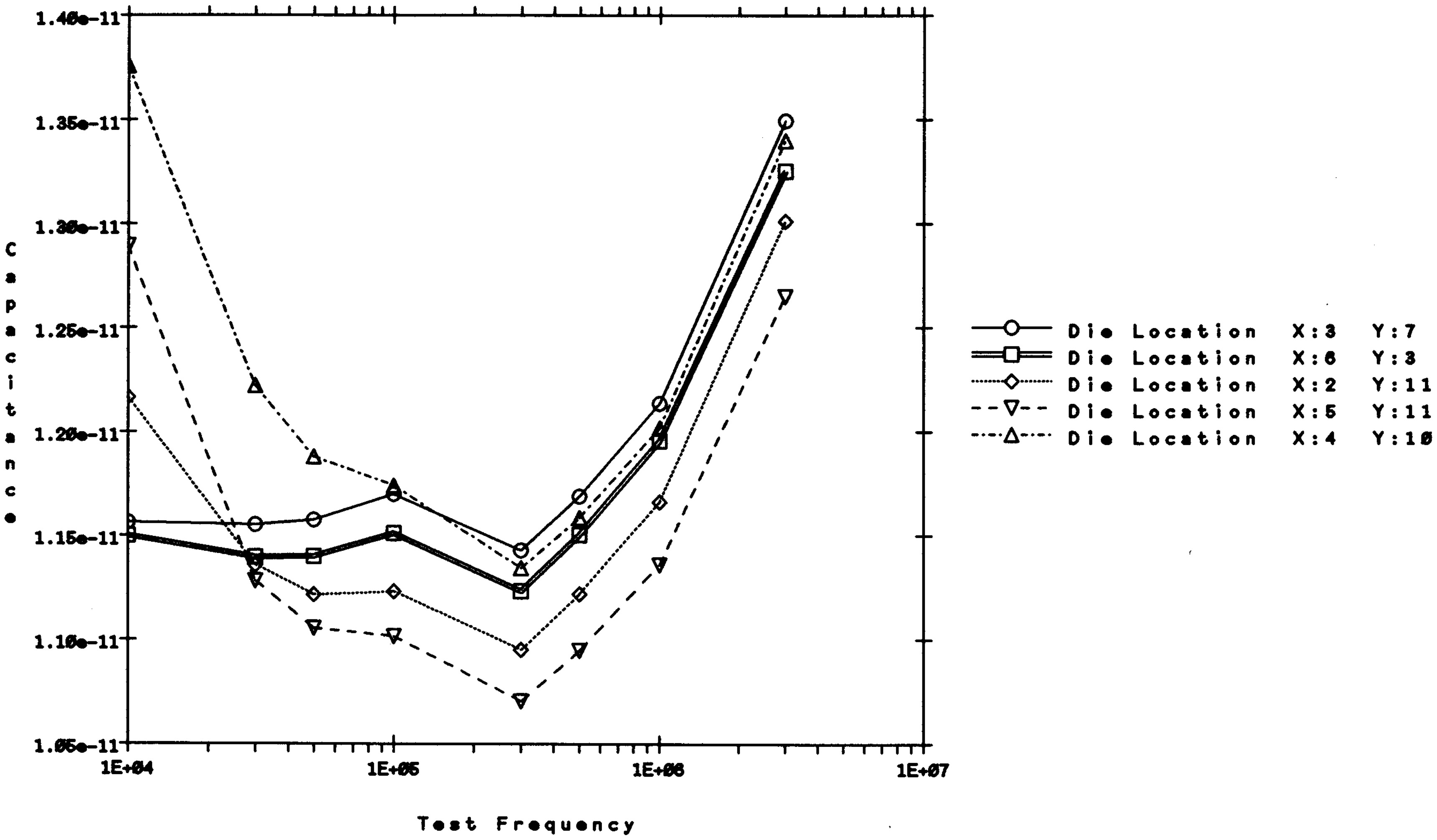

Moisture Penetration Experiment
Wafer 25, Run 15-820, 200 Hour HAST readout.
Metal 2, measured between Vss (29) & Bit Line Serp (28).
1.40e-11
1.35e-11
1.30e-11
1.25e-11
1.20e-11
1.15e-11
1.10e-11
1.05e-11
Capacitance
1E+04
1E+05
1E+06
1E+07
Test Frequency
Die Location X:3 Y:7
Die Location X:6 Y:3
Die Location X:2 Y:11
Die Location X:5 Y:11
Die Location X:4 Y:10
12 May 89, Maston

Fig 1. Schematic of Metal 1 and Metal 2 Array Defect Monitor on the I0441C test chip. The M2 comb/serpentine overlies and is orthogonal to the M1 comb/serpentine

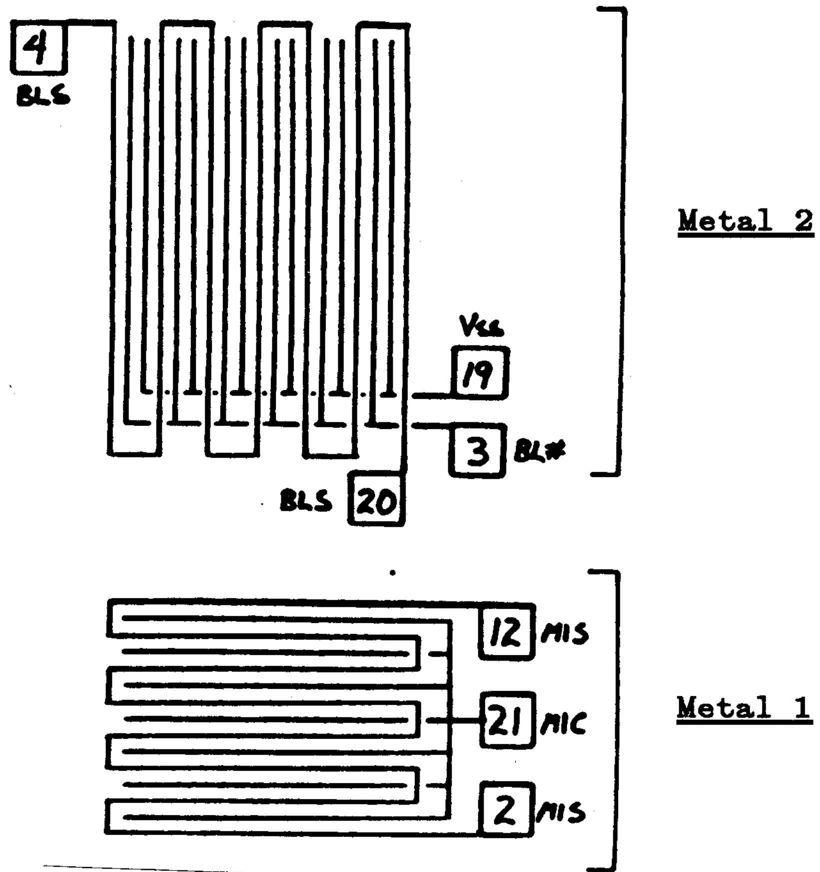

Fig. 1. Capacitance and dissipation factors at 100KHz vs time at 159/85 HAST. Top: M2 comb/serpentine. Bottom: M1 comb/serpentine. Oxynitride passivation, PSG ILD.

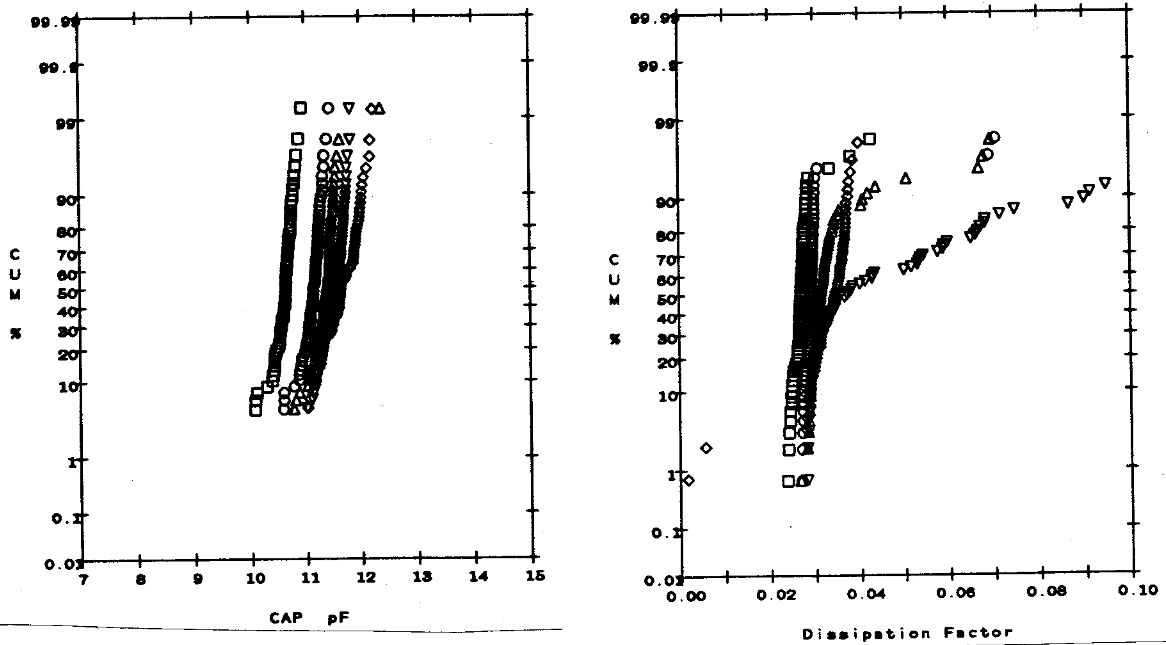

Metal 2 Array Defect Monitor
Vss / Serpentine

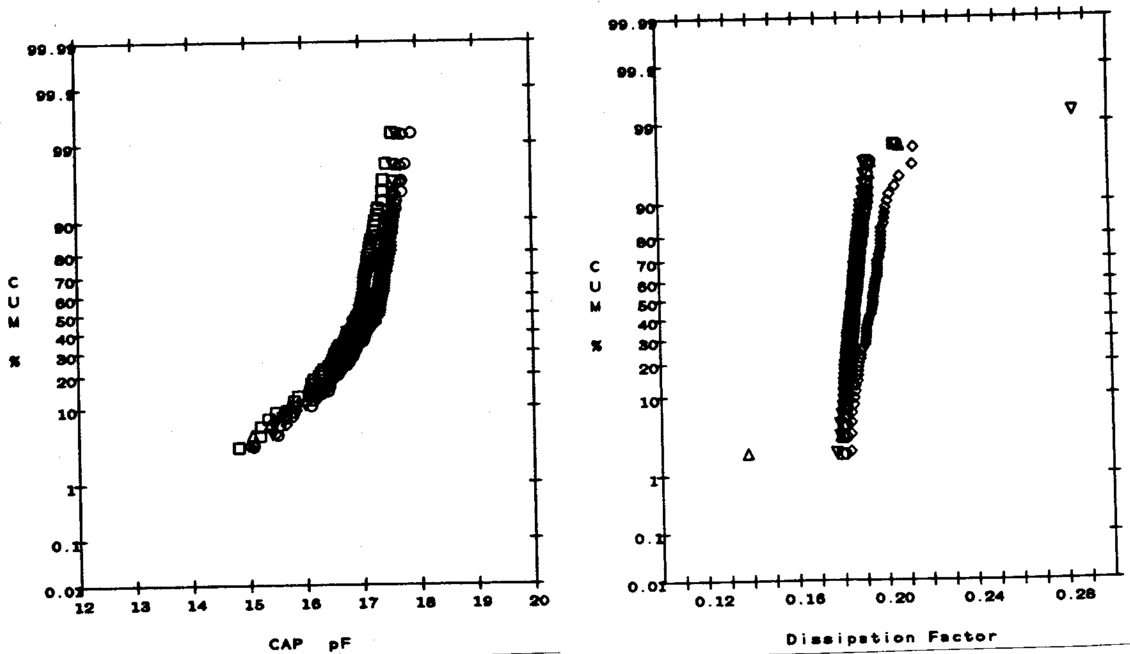

Metal 1, Array Defect Monitor
M1 Comb / M1 Serpentine

□ Pre-Stress.
○ HAST 80 Hrs.
△ HAST 160 Hrs.
▽ HAST 200 Hrs.
◇ HAST 280 Hrs.

Fig. 2. 100KHz dissipation factor of M2 comb/serpentine at 200 hours of 159/85 HAST. (See Fig. 1, top right.)

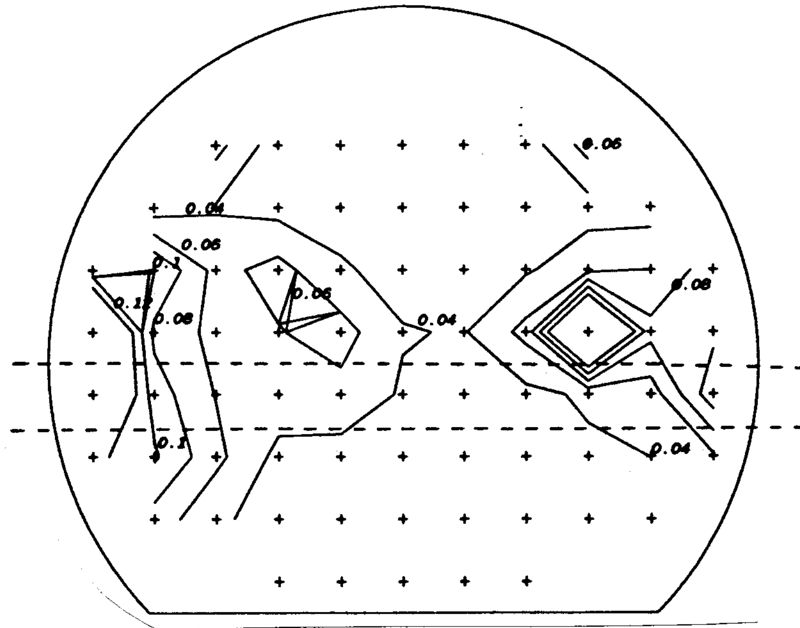

Fig. 3. 100KHz dissipation factor in 159/85 HAST, M2 comb/serpentine, section through wafer map in Fig. 2.

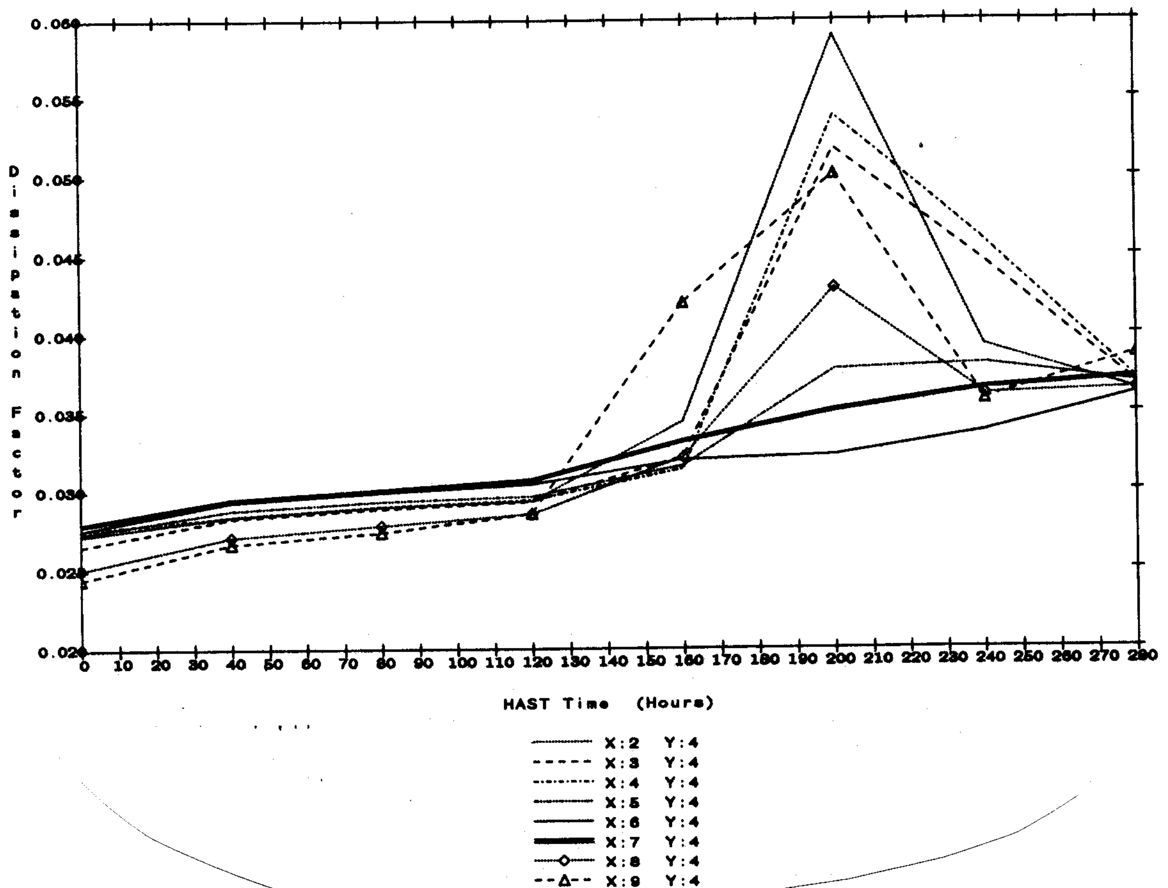

Fig. 4. Dissipation factor vs frequency for dice variously affected by moisture at 200 hours of 159/85 HAST. Data from same wafer as Figs. 1-3. Also shown is data from another unstressed wafer.

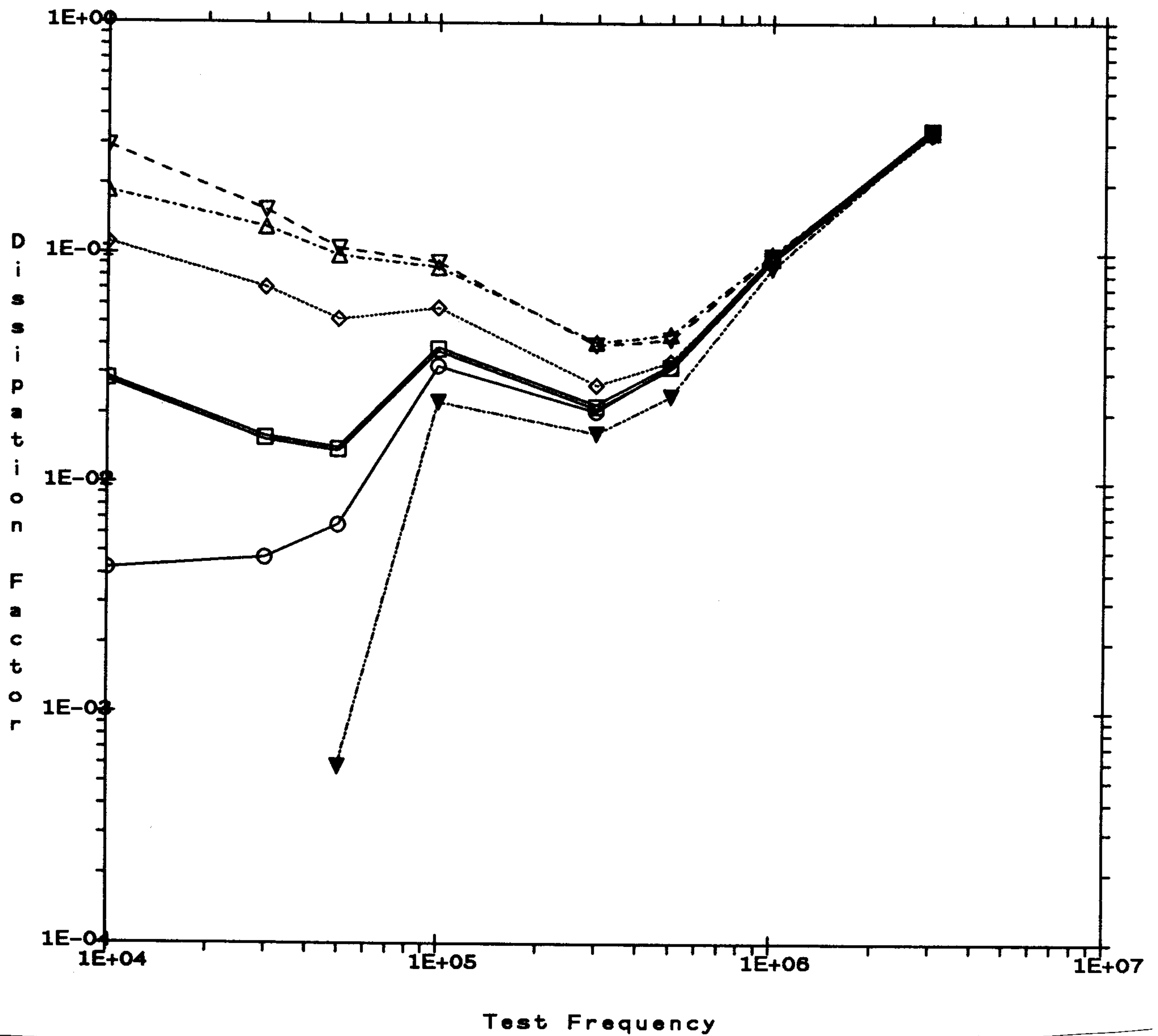

Die Location X:3 Y:7
Die Location X:6 Y:3
Die Location X:2 Y:11
Die Location X:5 Y:11
Die Location X:4 Y:10
Virgin Die W30 (29-841)

Fig. 5. Saturation and bake-recovery characteristic of several dice (packaged in open-lidded ceramic packages). 100KHz dissipation factor measurements on M2 comb/serpentine. Left: Changes in D during 159/85 HAST. Right: Recovery during 160C bake.